

Effects of endogenous cannabinoid anandamide on voltage-dependent sodium and calcium channels in rat ventricular myocytes.

Lina T. Al Kury¹, Oleg I. Voitychuk⁴, Keun-Hang Susan Yang⁵, Faisal T. Thayyullathil², Petro Doroshenko¹, Ali M. Ramez¹, Yaroslav M. Shuba⁴, Sehamuddin Galadari², Frank Christopher Howarth³, Murat Oz¹.

¹Laboratory of Functional Lipidomics, Department of Pharmacology, ²Department of Biochemistry, ³Department of Physiology, Faculty of Medicine and Health Sciences, UAE University, Al Ain, UAE, ⁴Bogomoletz Institute of Physiology and International Center of Molecular Physiology, National Academy of Sciences of Ukraine, Kyiv-24, Ukraine, ⁵Department of Biological Sciences, Schmid College of Science and Engineering, Chapman University, One University Drive, Orange, CA 92866, USA.

Address for correspondence:

Dr. Murat Oz,

Department of Pharmacology,

Faculty of Medicine & Health Sciences,

UAE University; P.O. Box 17666

Al Ain, Abu Dhabi, UAE

Phone: 00 971 3 7137523

Fax: 00 971 3 7672033

E-mail: murat_oz@uaeu.ac.ae

This article has been accepted for publication and undergone full peer review but has not been through the copyediting, typesetting, pagination and proofreading process, which may lead to differences between this version and the Version of Record. Please cite this article as doi: 10.1111/bph.12734

Abbreviations:

AP, action potential; AEA, anandamide; BTX, batrachotoxin; $I_{L,Ca}$, L-type Ca^{2+} current; metAEA, methanandamide; NAEs, N-acylethanolamines; PTX, pertussis toxin; I_{Na} , Na^{+} current; TTX, tetrodotoxin; VGSC, voltage gated sodium channel; VGCC, voltage gated calcium channel.

Accepted Article

Summary

Background and purpose: Endocannabinoid Anandamide (N-arachidonoyl ethanolamide; AEA) has been shown to cause negative inotropic and antiarrhythmic effects in ventricular myocytes.

Experimental approach: Whole-cell patch clamp technique and radioligand binding methods were used to test the effect of anandamide in rat ventricular myocytes.

Key results: In the presence of 1-10 μM AEA, suppression of both Na^+ and L-type Ca^{2+} channels was observed. Inhibition of Na^+ channels was voltage and pertussis toxin (PTX) - independent. Radioligand binding studies indicated that specific binding of [^3H] Batrachotoxin (BTX) to ventricular muscle membranes was also inhibited significantly by metAEA, a non-metabolized AEA analogue. In controls and in presence of 10 μM metAEA, B_{max} values were 76 ± 6 and 41 ± 4 fM, and K_{D} values were 32 ± 4 and 35 ± 3 nM, respectively. Further studies on L-type Ca^{2+} channels indicated that AEA potently inhibits these channels with IC_{50} of 0.1 μM in a voltage- and PTX- independent manner. AEA inhibited maximal amplitudes without affecting the kinetics of Ba^{2+} currents. MetAEA also inhibited Na^+ and L-type Ca^{2+} currents. Radioligand studies indicated that specific binding of [^3H]Isradipine, was inhibited significantly by metAEA. In controls and in presence of 10 μM metAEA, B_{max} were 146 ± 19 and 98 ± 24 fM/mg, and K_{D} values were 63 ± 4 and 86 ± 14 pM, respectively.

Conclusion: Results indicate that AEA inhibits the function of voltage-dependent Na^+ and L-type Ca^{2+} channels in rat ventricular myocytes in a manner independent of CB1 and CB2 receptor activation.

Keywords: Endocannabinoid, Anandamide, Na^+ channel, L-type Ca^{2+} channel, ventricular myocyte.

INTRODUCTION

Endocannabinoids are a group of polyunsaturated fatty acid-based compounds that mimic most of the effects tetrahydrocannabinol, the active ingredient of the marijuana plant *Cannabis sativa*. N-arachidonoyl ethanolamide (AEA) or Anandamide and 2-arachidonylglycerol are the most widely studied endogenous cannabinoids (Di Marzo *et al.*, 2005; Hanus and Mechoulam, 2010). In recent years, extensive research focusing on the biological actions of these compounds indicated that endocannabinoids have important regulatory roles in several physiological and pathological conditions (Pacher *et al.*, 2006; Di Marzo *et al.*, 2005; Pertwee *et al.*, 2010). It has been shown that endocannabinoid system consists of at least the endocannabinoid receptors (such as CB1 and CB2 cannabinoid receptors), the enzymes regulating the synthesis (such as phospholipase-D, and monoacylglycerol lipase), and the degradation (such as fatty-acid amide hydrolase and lipases) processes, and the proteins involved in their transport across the biological membranes (Di Marzo *et al.*, 2005; Pertwee *et al.*, 2010). CB₁ receptors are located in the brain and several peripheral tissues including the heart and the vasculature (Pertwee *et al.*, 2010). The CB₂ receptors, on the other hand, are expressed primarily in the immune system but recently their presence in the brain, myocardium, and smooth muscle cells have also been demonstrated (Pertwee *et al.*, 2010).

Recent studies suggest that endocannabinoids have important modulatory roles on the function of cardiovascular system under various pathological conditions, such as hypertension, myocardial infarction and heart failure [for recent reviews, (Batkai and Pacher, 2009; Montecucco and Di Marzo, 2012)]. AEA, the most studied endocannabinoid, has complex set of actions on cardiac functions. Experiments with AEA performed in isolated Langendorff rat hearts and in isolated, electrically stimulated human atrial appendages (Ford *et al.*, 2002; Bonz *et al.*, 2003) have revealed a negative

inotropic effect which may underlie its ability to decrease cardiac output as observed in studies performed *in vivo* (Wagner *et al.*, 2001). Moreover, AEA and other cannabinoids have been reported to have antiarrhythmic effects in *in vivo* animal models (Krylatov *et al.*, 2002; Ugdyzhekova *et al.*, 2001). In a recent study a weak protective effect of endocannabinoids during the late stages of ischemia has been suggested to be mediated by CB1 receptors (Andrag and Curtis, 2013). Another study reported that AEA potently inhibits the function of L-type Ca^{2+} channels by activating CB1 receptors in rat cardiomyocytes (Li *et al.*, 2009). However, electrophysiological mechanisms underlying these cardiac actions of AEA remain largely unknown. We hypothesized that some of the negative inotropic and antiarrhythmic actions of AEA can be mediated by the modulation of voltage-gated inward Na^{+} and Ca^{2+} channels. Thus, in the present study, using whole-cell patch clamp and radioligand binding methods, we investigated the actions of AEA on these major inward currents underlying the shape of the action potential in acutely dissociated rat ventricular myocytes.

Methods

Ventricular myocyte isolation: This study was carried out in accordance with the recommendations in the Guide for the Care and Use of Laboratory Animals of the National Institutes of Health. The work was performed with approval of Animal Research Ethics Committee of the College of Medicine and Health Sciences, UAE University. All studies involving animals are reported in accordance with the ARRIVE guidelines for reporting experiments involving animals (Kilkenny *et al.*, 2010; McGrath *et al.*, 2010). The original stocks of Wistar rats were purchased from Harlan Laboratories (Oxon, England). Animals were bred at our own Animal Facility from the original stock. The animals were housed in polypropylene cages (43 x 22.5 x 20.5 cm; six rats/cage) in climate and access controlled rooms (22-24 °C; 50 % humidity). The day/ night cycle was 12 h/12h. Food and water were provided *ad libitum*. The food was standard maintenance diet for rats purchased from Emirates Feed Factory (Abu Dhabi, UAE). Ventricular myocytes were isolated from adult male Wistar rats (264 ± 19 g) according to previously described technique (Howarth *et al.*, 2002). Briefly, the animals were euthanized using a guillotine and hearts were removed rapidly and mounted for retrograde perfusion according to the Langendorff method. Hearts were perfused at a constant flow of 8 ml g heart⁻¹ min⁻¹ and at 36-37 °C with a solution containing (mM): 130 NaCl, 5.4 KCl, 1.4 MgCl₂, 0.75 CaCl₂, 0.4 NaH₂PO₄, 5 HEPES, 10 glucose, 20 taurine, and 10 creatine set to pH 7.3 with NaOH. When the heart had stabilized perfusion was continued for 4 min with Ca²⁺-free isolation solution containing 0.1 mM EGTA, and then for 6 min with cell isolation solution containing 0.05 mM Ca²⁺, 0.75 mg/ml collagenase (type 1; Worthington Biochemical Corp, USA) and 0.075 mg/ml protease (type X1 V; Sigma, Germany). Ventricles were excised from the heart, minced and gently shaken in collagenase-

containing isolation solution supplemented with 1 % BSA. Cells were filtered from this solution at 4 min intervals and resuspended in isolation solution containing 0.75 mM Ca^{2+} .

Measurement of Na^+ and L-type Ca^{2+} Currents: Currents were measured using whole-cell patch clamp technique and recorded with an Axopatch 200B amplifier (Molecular Devices, Downington, PA, USA) linked to an A/D interface (Digidata 1322; Molecular Devices). Currents were filtered at 5 kHz and acquired using Clampex 8.2. Patch pipettes were fabricated from filamented GC150TF borosilicate glass (Harvard Apparatus, Holliston, MA, USA) on a horizontal puller (Sutter Instruments Co., Novato, CA). Electrode resistances ranged from 2.0 to 3.0 $\text{M}\Omega$, and seal resistances were 1-5 $\text{G}\Omega$. After giga seal formation, the membrane was ruptured with gentle suction to obtain whole cell voltage-clamp configuration. In recording of Na^+ currents, cells were held at -80 mV and were depolarized with 50 ms pulses from -80 mV to +70 mV in 10 mV increments. Extracellular solution for recordings of Na^+ currents consisted of (in mM): 100 TEACl, 40 NaCl, 10 glucose, 1 MgCl_2 , 5 CsCl, 0.1 CaCl_2 , 1 NiCl_2 , and 10 HEPES (adjusted to pH 7.3 with CsOH). Intracellular solution contained (in mM) 135 CsCl, 5 NaCl, 10 EGTA, 10 HEPES and 1 MgATP (adjusted to pH 7.25 with CsOH). For recording of Ca^{2+} currents, data were elicited from a holding potential of -50 mV to membrane potentials ranging from -70 mV to +70 mV in 10 mV increments every 300 ms. The whole-cell bath solution contained (in mM): 95 NaCl, 50 TEACl, 2 MgCl_2 , 2 CaCl_2 , 10 HEPES and 10 glucose (adjusted to pH 7.35 with NaOH). The pipette solution contained (in mM): 140 CsCl, 10 TEACl, 2.0 MgCl_2 , 2 HEPES 1 MgATP and 10 EGTA (adjusted to pH 7.25 with CsOH). Experiments were performed at room temperature (22–24 °C). Changes of external solutions and application of drugs were performed using a multi-line perfusion system with a common outflow connected to recording chamber. Electrophysiological data were analyzed using pClamp 10.2 (Molecular Devices, Union City, CA) and Origin 7.0 (OriginLab Corp., Northampton, MA) software. The amplitudes of the currents were normalized to the cell

membrane capacitance to provide current densities (nA/pF). The $G_{i/o}$ protein blocker pertussis toxin (PTX; 2 μ g/ml) was purchased from Sigma. Cells were incubated with PTX for 3 h at 37°C (control cells to this group were incubated in the same conditions with distilled water only).

Radioligand Binding Studies with [³H]BTX-B: Myocytes were prepared daily from adult rat

ventricles with a yield of 8-10 x 10⁶ myocytes/heart, of which 75-80% were viable rod-shaped striated cells. Cells were collected by gentle centrifugation (40 x g) for 5 min, rinsed twice with incubation solution, stored at room temperature (21-23 °C) in incubation solution and used within 30 min.

Myocytes (5 x 10⁵ per assay) in 200 μ l of incubation buffer (minimal essential medium (MEM) with 50 μ M CaCl₂) were incubated (in duplicate or triplicate in polypropylene centrifuge tubes) with 1 μ M sea anemone toxin (ATX), 100 μ M tetrodotoxin (TTX), and various concentrations of [³H]BTX-B for 60 min at 37°C in the cell-culture incubator. TTX was added to prevent depolarization induced by Na⁺ influx induced by the toxins (Sheldon *et al.*, 1986). Various concentrations of metAEA dissolved in ethanol were added in volumes of 3-5 μ l to the incubation buffer (The same volumes of ethanol were added to the control samples). These volumes of ethanol had no effect on the [³H]BTX-B binding).

Assays were done in parallel with tubes containing 0.4 mM aconitine to define nonspecific binding. At the end of the 60-min incubation period, 150 μ l of the reaction mixture (cell suspension) from each sample were filtered through a Whatman GF/C 25-mm fiber-glass filter under vacuum. The reaction was terminated by adding 10 ml of Krebs-Henseleit-BSA buffer (127 mM NaCl, 2.3 mM KCl, 1.30 mM KH₂PO₄, 1.2 mM MgSO₄, 25 mM NaHCO₃, 10 mM glucose, 50 μ M CaCl₂, 1% BSA) equilibrated with 95% O₂ + 5% CO₂ and incubated at 37 °C for 1 min, then filtered through a Whatman GF-C 24-mm fiber-glass filter and washed four times with 5 ml of rinse buffer (25 mM Tris-Cl, pH 7.4, 130 mM NaCl, 5.5 mM KCl, 0.8 mM MgSO₄, 5.5 mM glucose, 50 μ M CaCl₂). The filters were then dried and counted in Econofluor-2 scintillation fluid (PerkinElmer Inc., Waltham, MA, USA) and assessed for

cell-bound radioactivity in a Beckman LS-6000SC liquid scintillation counter. (The counting efficiency was 48-50%). Specific binding was calculated as the difference between total and nonspecific binding.

Under these conditions nonspecific binding was 20-30% of total binding at 30 nM [³H]BTXB. The dissociation constant (K_d) and maximal binding (B_{max}) were determined by Scatchard analysis.

Specific activity of [³H]BTX-B was 41.3 Ci/mmol; 1 Ci = 37 GBq) was from New England Nuclear.

Sea anemone toxin and TTX were obtained from Sigma-Aldrich. metAEA was dissolved weekly in ethanol at the concentration of 10 mM and stored at -20°C.

Preparation of cardiac muscle membranes: Cardiac membranes were prepared from the heart of adult male Wistar rats by some modifications of previously described methods (Dunn, 1989; Oz *et al.*, 2000). Briefly, rat heart was minced with scissors and washed two times with ice-cold binding buffer to remove extraneous blood. The tissue (one heart in a 50-ml) was placed in plastic centrifuge tube containing 10 ml ice-cold buffer (50 mM Tris-Cl, pH 7.2) and homogenized on ice by two 5-sec bursts in a Polytron homogenizer at setting 5. The solution was decanted to a motor-driven 10-ml glass-Teflon homogenizer and homogenized on ice by 10 passes at setting 8. The homogenate was filtered through four layers of cheesecloth (to remove tissue debris) into a clear 50-ml centrifuge tube and centrifuged for 45 min at 45,000 × g, 4°C. The pellet was suspended in 5 ml ice-cold binding buffer for each rabbit heart by homogenizing the pellet five times on ice with a motor-driven 10-ml glass-Teflon homogenizer at setting 5. Membrane protein concentration was determined using the Bradford method using BSA as a standard. The membranes were diluted in binding buffer to 1 mg protein/ml and store in 5-ml aliquots at -70°C.

Radioligand Binding Studies with [³H]Isradipine: Experiments on the binding of [³H]Isradipine (Specific activity 58.6 Ci /mmol, New England Nuclear, Chadds Ford, PA, USA) were conducted similar to our earlier studies (Oz *et al.*, 2000). Briefly, aliquots of membranes (0.1 mg) were added to

different concentrations of radiolabeled ligand to give a final concentration of 0.02 mg/ml membranes in a total volume of 0.8 ml. After 60 min incubation at room temperature, 0.4 ml aliquots of each sample were filtered under vacuum through Watman GF/C filters and rapidly washed with 5 ml of ice-cold assay buffer. The filters were dried and extracted in 5 ml of Hydroflour™ (National Diagnostics, St. Louis, MO, USA) scintillation fluid before counting for ³H. Triplicate 50-μl samples of the incubation mixtures were also counted directly for estimations of total binding. Nonspecific binding was estimated from parallel measurements of binding in the presence of 5 μM unlabeled nifedipine. MetAEA, AEA, AM251, and AM630 were purchased from Tocris (Ellisville, MO, USA). All other materials mentioned were purchased from Sigma-Aldrich (St. Louis, MO, USA). In patch clamp experiments, ethanol concentrations in control and in presence of AEA, metAEA and AM251 were in the range of 0.007- 0.07 % v/v. AM630 was dissolved in DMSO and the final concentration for DMSO used in the experiments did not exceed 0.007% (v/v). Stock solutions of AEA, AM251 and AM630 were kept at -20 °C until their use. Ethanol at the concentration range used in our experiments had no effect on the specific binding of [³H]BTX-B and [³H]Isradipine.

Data Analysis: The results of the experiments were expressed as mean ± standard error of the mean (S.E.M.). Statistical analysis was performed using the paired *t*-test (within the same cell analysis).

Statistical significance among groups was determined using one way ANOVA followed by Benferonni Post-hoc analysis. Statistical analysis of the data was performed using Origin 7.0 software (OriginLab Corp., Northampton, MA) and IBM SPSS statistics version 20. On all graphs (*) denotes statistical significance with *P*<0.05, between specified values, or if not specified to the respective control.

RESULTS

The passive properties of the ventricular cells from controls were not significantly different from those of the AEA treated cells. Resting membrane potentials (mean \pm SEM) were -76.2 ± 1.3 and -78.3 ± 1.5 mV in control (n=38) and AEA treated (n=53) myocytes, respectively. The mean cell capacitance in the control group was 117.2 ± 14.7 pF, whereas in the AEA treated cells was 108.3 ± 12.1 pF. The input resistance (measured close to the resting potential) was 72.4 ± 16.5 M Ω in the control cells and 79.3 ± 17.8 M Ω in AEA-treated cells. In control cells, these passive membrane properties were not altered significantly in experiments lasting up to 25 to 30 min. In 18 control cells measured, resting membrane potentials, cell capacitance, and input resistance after 25 min of experiment were -74.8 ± 3.4 mV, 109.6 ± 14.3 pF, and 81.2 ± 14.3 M Ω , respectively. These values were not significantly different from control values obtained within the first 5 min of patch-clamp experiment (n=18; paired t-test, $P > 0.05$). Characteristics (threshold, maximal, and reversal potentials) of current-voltage relationship remained stable during the experiments.

Effects of AEA on voltage-dependent Na⁺ channels:

Previous studies have indicated that AEA has significant antiarrhythmic effects suggesting that this compound may affect voltage activated inward Na⁺ (I_{Na}) and Ca²⁺ ($I_{L,Ca}$) currents of ventricular myocytes. To verify these possibilities, we have conducted a series of experiments under conditions that enable reliable isolation of either I_{Na} or I_{Ca} in voltage-clamp mode. In the first set of experiments, I_{Na} was typically elicited by pulses from -80 mV to -20 mV for 50 ms. Figure 1A shows recordings of I_{Na} in ventricular myocytes before, during and after application of $10 \mu\text{M}$ AEA. The effect of AEA was detectable at 2-3 min and reached a steady-state level within 10-15 min (Fig. 1B). The recovery was

partial during the experiments lasting up to 25 to 30 min (Fig. 1B). In our studies, AEA was dissolved in ethanol, and therefore we have tested the effect of ethanol as a vehicle. In agreement with earlier studies (Danziger *et al.*, 1991; Bebarova *et al.*, 2010), our results indicated that maximal amplitudes of I_{Na} were altered after 10 min vehicle application in experiments lasting up to 20 to 25 min. Due to the effect of vehicle, we have tested each concentration of AEA and vehicle separately and plotted the concentration response curve after the subtraction of vehicle effect (Supplement Figure 1). The effect of increasing AEA and corresponding ethanol concentrations and corrected concentration-response curve were presented in supplement Figure 1. In order to exclude the possibility of the involvement of degradation products of AEA in the inhibition of Na^+ current, the effect of 10 μM metAEA was tested. metAEA caused a significant inhibition of Na^+ currents (36 ± 4 % inhibition of controls; $n=5$; paired t-test).

With 40 mM Na^+ outside and Cs^+ as the major intracellular cation, inward I_{Na} in response to incremental step depolarizations (V_m , 10 mV increment) applied from a holding potential $V_h = -80$ mV started to activate at $V_m = -50$ mV, and reached maximal amplitude at $V_m = -30$ mV. At more positive potentials the inward current decreased reversing its direction at an apparent reversal potential (V_{rev}) of around +60 mV. Traces of I_{Na} in the absence and presence of 10 μM AEA were presented in Figure 1C. AEA inhibited I_{Na} without causing significant changes in the I - V relationship. The current-voltage (I - V) relationship for I_{Na} was illustrated in Figure 1D. AEA inhibited I_{Na} without changing the threshold, peak and reversal potentials.

Steady-state activation (SSA) curves of I_{Na} before and after AEA application were derived by fitting the respective I - V relationships with the product of Boltzmann and Goldman-Hodgkin-Katz (GHK) equations of which the first one describes voltage-dependence of SSA, and the second one the current through open channels. This allowed us to determine if AEA influences the parameters of I_{Na}

SSA-the voltage of half-maximal activation ($V_{1/2}$) and slope factor (k). In controls, $V_{1/2}$ and k values were -45.2 mV and 7.1 mV, respectively. In the presence of 10 μ M AEA, $V_{1/2}$ and k values were -42.3 mV, and 7.5 mV (Fig. 2A). There were no statistically significant differences between controls and in the presence of AEA (ANOVA, $n=8-10$; $P>0.05$).

In order to determine if AEA influences the properties of voltage gated sodium channels (VGSCs) inactivation, we compared steady-state inactivation (SSI) dependencies of I_{Na} in the absence and presence of AEA. SSI-curves were acquired using a standard voltage protocol consisting of prolonged (400 ms) conditioning pre-pulse to various V_m in the range of -100 mV to +70 mV which was immediately followed by the constant I_{Na} -activating test pulse to $V_m = -20$ mV. SSI-dependency was plotted as normalized amplitude of I_{Na} at $V_m = -20$ mV against the value of conditioning V_m (normalization was performed to the amplitude of I_{Na} at conditioning $V_m = -100$ mV). The fit of the obtained data points using the Boltzmann equation (Fig. 2B) has indicated that under control conditions SSI of I_{Na} is $V_{1/2} = -70.2$ mV and $k = 5.8$ mV, and in the presence of 10 μ M of AEA, $V_{1/2} = -81.4$ mV and $k = 5.1$ mV. Thus, AEA induced a significant hyperpolarizing shift in the voltage-dependence of SSI of cardiac VGSCs (-11.4 mV; paired t -test, $P < 0.05$). Comparison of I_{Na} currents in the absence and presence of AEA revealed noticeable acceleration of the current's inactivation kinetics by AEA. Quantification of the time constant of I_{Na} inactivation (τ_i , Fig. 2C) by fitting the currents' decay phase with exponential functions showed that AEA (10 μ M) significantly reduced τ_i in the range of V_m between -50 mV and +20 mV (Fig. 2C).

The rat heart has been shown to express CB1 and CB2 receptors (Bouchard *et al.*, 2003). Therefore it was likely that the effect of AEA is mediated by the activation of these receptors. For this purpose we have chosen two antagonists (AM251 and AM630) for their relative selectivity for CB1 versus CB2 receptor (Lan *et al.*, 1999; Ross *et al.*, 1999) defined in accordance with the nomenclature

of the Guide to Receptors and Channels (Alexander *et al.*, 2011). In the presence of 0.3 μM AM251, a CB1 antagonist with K_i of 7.5 nM (Lan *et al.*, 1999) and 0.3 μM AM630, a CB2 antagonist with K_i of 32.1 nM (Ross *et al.*, 1999), AEA (10 μM) inhibition of I_{Na} remained unaltered (n=6-8, data not shown). Since the known cannabinoid receptors CB1 and CB2 [for a review (Pertwee *et al.*, 2010)] are coupled to pertussis toxin (PTX) sensitive $G_{i/o}$ type G-proteins, we have tested whether the inhibitory effect of AEA on I_{Na} can be modulated by PTX pretreatments. Our results show that the extent of the inhibitory effect of AEA on the maximal amplitudes of I_{Na} was not affected by PTX pretreatment (Fig. 2D). There were no statistically significant difference in the % inhibition by AEA in control and PTX-treated groups (n=6-8; ANOVA; $P>0.05$). In positive control experiments, PTX, as it has been reported earlier (Zhang *et al.*, 2005) effectively attenuated the inhibitory actions of BRL-37344, a β_3 adrenergic receptor agonist, on L-type voltage-gated Ca^{2+} currents recorded in ventricular myocytes (supplement Figure 2). These results indicate that G-proteins are functionally coupled to their target receptors.

Effect of metAEA on [^3H]BTX-B binding:

The results of electrophysiological experiments suggest that AEA can directly interact with VGSCs. For this reason, we have conducted radioligand binding experiments to test the possibility of direct interaction between AEA and VGSCs in cardiomyocytes. Binding of [^3H] Batrachotoxin in cardiomyocytes (Sheldon *et al.*, 1986; Kang and Leaf, 1996) and neuronal structures (Postma and Catterall, 1984) has been well characterized in earlier investigations. In this study, due to long incubation times (up to 60 min), we have tested the effect of methanandamide (metAEA), a non-hydrolysable AEA analogue (Abadji *et al.*, 1994), to avoid likely confounding effects of degradation products and oxygenated metabolites on the specific binding of [^3H]batrachotoxinin A-20 α -benzoate ([^3H]BTX-B) in rat ventricular cardiomyocytes.

Equilibrium curves for the binding of [^3H]BTX-B, in the presence and absence of metAEA are presented in Figure 3A (n= 8-11). At a concentration of 10 μM , metAEA caused a significant inhibition of the specific binding of [^3H]BTX-B. In controls and in presence of 10 μM metAEA, maximum binding activities (Bmax) were 76 ± 6 and 41 ± 4 fM, and K_D values were 32 ± 4 and 35 ± 3 nM, respectively. There was a statistically significant difference between control and metAEA treated groups with respect to Bmax values (n=8-11; ANOVA; $P < 0.05$). Effect of metAEA on saturation binding was further analyzed by Scatchard analysis (Fig. 3B), which yielded a Bmax of 92 fmol and a Kd of 21 nM [^3H]BTX-B for controls and a Bmax of 43 fmol and a Kd of 24 nM for cells treated with metAEA. To further determine the effects of metAEA on the binding of [^3H]BTX-B to cardiac Na^+ channels, myocytes were incubated with [^3H]BTX-B in the presence of increasing metAEA concentrations. The results indicated that the metAEA inhibited the specific binding of [^3H]BTX-B in a dose-dependent manner with an IC_{50} of 8.6 μM and slope of 1.1 (Fig. 3A). We have also investigated the effect of CB receptor antagonists AM251 (1 μM) and AM630 (1 μM) on the specific binding of 10 nM [^3H]BTX-B. Results presented in Figure 3D indicate that the effect of metAEA (10 μM) on the specific binding of [^3H]BTX-B was not significantly altered in the presence AM251 or AM630 (compared to AEA alone, n=7-11; ANOVA; $P > 0.05$). Incubation with AM251 or AM630 alone did not significantly alter the specific [^3H]BTX-B binding from cardiac muscle membranes (ANOVA; n=7-11; $P > 0.05$)

Effect of AEA on L-type Ca^{2+} currents:

We have also investigated the effect of AEA (1 μM) on the L-type Ca^{2+} currents ($I_{L,\text{Ca}}$). Figure 4A shows a typical record of $I_{L,\text{Ca}}$ elicited by applying a single 300 ms voltage pulse to +10 mV from a holding potential of -50 mV in rat ventricular myocyte before and after 10 min superfusion with 1 μM AEA. Time course of the effect of AEA on the density of $I_{L,\text{Ca}}$ was presented in Figure 4B. Current

density of $I_{L,Ca}$ were also altered after 10 min vehicle application in experiments lasting up to 20 to 25 min. Effects of increasing AEA and corresponding ethanol concentrations on $I_{L,Ca}$ and corrected concentration-response curve were presented in supplement Figure 3. The effect of 1 μ M metAEA was also tested. metAEA caused a significant inhibition of Ca^{+2} currents (46 ± 4 inhibition of controls; $n=5$; paired t-test).

The effects of AEA were also investigated on the biophysical properties of $I_{L,Ca}$ in rat ventricular myocytes. $I_{L,Ca}$ was recorded in the presence of intracellular Cs^+ and extracellular TEA^+ to suppress K^+ currents while retaining 95 mM Na^+ in the extracellular solution. Elimination of contaminating Na^+ current during recording of $I_{L,Ca}$ was achieved by applying voltage step-pulses from relatively depolarized V_h of -50 mV, which produced steady-state I_{Na} inactivation (Voitychuk *et al.*, 2012). As evident from original recordings and I - V relationships (Fig. 4C, D), $I_{L,Ca}$ had much slower kinetics in response to step depolarization and activated at more positive potentials than I_{Na} : it started to appear at $V_m = -30$ mV, reached maximum at around $V_m = +10$ mV, and decreased at higher voltages approaching zero at about $V_m = +60$ mV (Fig.4D).

AEA also produced a depolarizing shift of $I_{L,Ca}$ SSA by 12.6 mV (i.e., from control value $V_{1/2} = -9.4 \pm 0.3$ mV to $V_{1/2} = +3.2 \pm 0.2$ mV in the presence of AEA) and hyperpolarizing shift of $I_{L,Ca}$ SSI by 4.3 mV (i.e., from control value $V_{1/2} = -18.9 \pm 0.1$ mV to $V_{1/2} = -23.2 \pm 0.1$ mV in the presence of AEA) with little influence on the slopes of respective dependencies ($k=7.2 \pm 0.4$ mV and $k=-5.3 \pm 0.3$ mV for the control activation and inactivation, respectively, vs. $k=6.9 \pm 0.3$ mV and $k=-5.1 \pm 0.2$ mV for the AEA-modified activation and inactivation, respectively), which altogether resulted in the notable reduction of $I_{L,Ca}$ “window current” responsible for the stationary Ca^{2+} entry in the range of membrane potentials from -40 mV to +10 mV (Fig. 5A, B). Thus, the mechanism of AEA action on cardiac L-type voltage gated calcium channel (VGCC) most likely involves influence on channel gating that reduces

“window current” as well as partial blockade of the ion-conducting pathway that decreases current amplitude. In time matching controls measured after 10 min of ethanol application, activation and inactivation parameters was not significantly different compared to time-matched controls (without ethanol application after 10 to 15 min of patching time). $V_{1/2}$ values for activation and inactivation were -10.3 ± 0.4 mV and -20.6 ± 0.7 for controls, and -9.7 ± 0.6 mV and -19.6 ± 0.8 in the presence of 0.007% (1.5 mM) ethanol, respectively (n=7-9; ANOVA, $P>0.05$).

In line with earlier reports (Soldatov *et al.*, 1998), kinetic analysis of $I_{L,Ca}$ currents were fit to double-exponential function with fast (τ_f) and slow (τ_s) inactivation time constants. Comparison of $I_{L,Ca}$ currents in the absence and presence of AEA revealed noticeable acceleration of the current's inactivation kinetics by AEA. Quantification of the time constants of $I_{L,Ca}$ inactivation showed that AEA (1 μ M) significantly reduced τ_i in the range of V_m -30 mV and +10 mV (Fig. 5C).

In earlier electrophysiological studies, sidedness of AEA actions on various ion channels has been reported (Oz, 2006). For this reason, we have tested the effect of intracellular application of AEA by including AEA (1 μ M) inside the patch electrode (Fig. 5D). The extent of AEA inhibition (compared after 15 min of AEA exposure) was not significantly different between intracellular and extracellular AEA applications (ANOVA; n=11-14; $P>0.05$). We have also conducted experiments with URB597, a potent inhibitor of FAAH which is the enzyme that hydrolyzes AEA (incubation of 1 μ M URB597 for 45 min at 37 °C versus controls incubated with 0.007 % ethanol alone for 45 min at 37 °C). Our results indicate that the effect of 1 μ M AEA on L-type Ca^{2+} currents remained unaltered in URB597-incubated cells. The extent of AEA inhibition was in the presence and absence of URB597 treatment was 35 ± 4 % and 32 ± 3 %, respectively (n=5-7; ANOVA, $P>0.05$).

In the next series of experiments, we tested if the modulation of Ca^{2+} binding site can mediate the effect of AEA on the inactivation kinetics of L-type VGCCs. For this purpose, we have replaced extracellular Ca^{2+} with Ba^{2+} and tested the effect of AEA on Ba^{2+} currents (I_{Ba}) through L-type VGCCs. In line with earlier studies (Soldatov *et al.*, 1998), inactivation of I_{Ba} fit to mono-exponential decay function (Fig. 6A) with significant voltage-dependency. In the presence of AEA, inactivation time constant (Fig. 6A and 6B), and the maximal amplitudes of I_{Ba} were significantly inhibited compared to control values (paired *t*-test; $n=7$; $P<0.05$).

We have also investigated whether the inhibitory effects of AEA on L-type VGCCs are mediated by the activation of cannabinoid receptors. Since the known cannabinoid receptors CB1 and CB2 [for a review (Pertwee *et al.*, 2010)] are coupled to pertussis toxin (PTX) sensitive $G_{i/o}$ type G-proteins, we have tested whether the inhibitory effect of AEA on L-type VGCCs can be modulated by PTX pretreatments. Our results show that the inhibitory effect of AEA on the maximal amplitudes of $I_{\text{L,Ca}}$ was not affected by PTX pretreatment (Fig. 6C). We have conducted further experiments in which 1 mM GTP was included in the pipette solution. In the presence of GTP, AEA (10 min bath application) continued to inhibit L-type Ca^{2+} currents to 62 ± 4 % of controls ($n=6$). Furthermore, in the presence of 0.3 μM AM251, a CB1 antagonist with K_i of 7.5 nM (Lan *et al.*, 1999) and 0.3 μM AM630, a CB2 antagonist with K_i of 32.1 nM (Ross *et al.*, 1999), AEA (1 μM) inhibition of $I_{\text{L,Ca}}$ remained unaltered (Fig. 6D). There were no statistically significant difference in the % inhibition by AEA among AEA, AEA+AM251, and AEA+AM630-treated groups ($n=6-9$; ANOVA; $P>0.05$). Application of AM251 or AM630 alone did not have a significant effect on the amplitudes of $I_{\text{L,Ca}}$ (Fig. 6D) ($n=8$; Paired *t*-test; $P>0.05$).

Effect of metAEA on [³H]Isradipine binding:

In cardiac tissue, AEA is hydrolyzed to arachidonic acid (AA), and AA is known to inhibit the function of cardiac L-type Ca²⁺ channels and cause negative inotropic actions (Li *et al.*, 2009); for a review of earlier studies, (Oz, 2006). Therefore it was possible that AA, rather than AEA, interacts with L-type Ca²⁺ channels. For this reason, we tested the effect of metAEA, the metabolically stable chiral analogue of AEA which is resistant to hydrolytic inactivation by fatty acid amide hydrolase (Abadji *et al.*, 1994) on the specific binding of [³H]Isradipine. Equilibrium curves for the binding of [³H]Isradipine, in the presence and absence of the metAEA are presented in Figure 7A (n= 8-11). At a concentration of 10 μM, metAEA caused a significant inhibition of the specific binding of [³H]Isradipine. In controls and in presence of 10 μM AEA, Maximum binding activities (Bmax) were 126 ± 19 and 58 ± 24 fM/mg protein, and K_D values were 75 ± 12 and 86 ± 14 pM, respectively. There was a statistically significant difference between control and metAEA treated groups with respect to Bmax values (*P*<0.05, ANOVA, n=8-11). Effect of metAEA on saturation binding was further analyzed by Scatchard analysis (Fig. 7B), which yielded a Bmax of 178 ± 19 fmol/mg protein and a K_d of 78 ± 8 pM [³H]Isradipine for controls and a Bmax of 68 ± 9 fmol/mg protein and a K_d of 76 ± 8 pM for membranes treated with metAEA. The effect of increasing metAEA concentrations was also investigated on the specific [³H]Isradipine binding from cardiac muscle membranes (Fig. 7C). In the concentration range used (0.1 to 30 μM), metAEA caused a significant inhibition of the specific binding of [³H]Isradipine. The values for IC₅₀ and slope factor for metAEA were 3.6 μM and 1.4, respectively.

Effects of CB receptor antagonists on the specific [³H]Isradipine binding from cardiac muscle membranes, were also investigated. Compared to controls, inhibitory effect of metAEA (10 μM) on the

specific binding of [³H]Isradipine was not altered by incubation (30 min) with AM251 or AM630 (1 μM) (Fig. 7D) (ANOVA; n=8-10; *P*>0.05). Incubation with AM251 or AM630 alone did not significantly alter the specific [³H]Isradipine binding from cardiac muscle membranes (ANOVA; n=8-10; *P*>0.05)

Accepted Article

DISCUSSION:

The results of this study indicate for the first time that previously reported actions of AEA on cardiac muscle contractility (negative inotropic effect) and the action potential (AP) configuration involves direct inhibition of voltage-dependent Na^+ and Ca^{2+} channels in ventricular myocytes. Actions of endocannabinoids on cardiovascular system influence multiple organ systems and involve complex set of cellular and molecular mechanisms (Malinowska *et al.*, 2012; Randall *et al.*, 2004). In addition to cannabinoid receptor-mediated actions, several other factors such as the activation of autonomic reflexes, the presence of endothelial cells and fatty-acid based metabolic products have been reported to contribute to the complexity of endocannabinoid actions on the heart. On the other hand, acutely dissociated ventricular myocytes have several advantages over *in-vivo* and traditional *in-vitro* conditions, since it excludes the influences of reflex pathways, autonomic nerve endings, neurotransmitter uptake system, gap-junction connections, and coronary perfusion status.

In our experiments, AEA caused a significant reduction in the maximal amplitudes of both Na^+ and Ca^{2+} currents. Inhibitory effect of AEA, on VGSC, which is the major inward current during the upstroke (phase 0) of the AP is in agreement with our recently published current-clamp studies (Al Kury *et al.*, 2014) indicating that AEA decreases the amplitude and initial rate of rise of the AP in ventricular myocytes. The results suggest that the effect of AEA on VGSC is not mediated by CB1 or CB2 cannabinoid receptors. Furthermore, radioligand binding experiments indicate that AEA can interact directly with VGSC in ventricular myocytes. In cardiac muscles, VGSCs are almost exclusively represented by their TTX-resistant Nav1.5 isoform (gene SCN5A; (Catterall *et al.*, 2005a)). Therefore, the changes in the biophysical properties of I_{Na} by AEA, namely induction of the hyperpolarizing shift in the voltage-dependence of its steady-state inactivation (SSI) can be attributed to their effects on Nav1.5 channel gating.

A hyperpolarizing shift of the SSI indicates that a higher proportion of VGSCs would be inactivated at resting membrane potential and therefore substantially fewer channels would be available for activation, resulting in decreased amplitude and rate of rise during the upstroke of the AP.

Our radioligand studies indicated that [³H]BTX-B binding was inhibited by AEA in an allosteric manner. The binding site for [³H]BTX-B has also been shown to interact allosterically with local anesthetics and class I antiarrhythmics (Sheldon *et al.*, 1994). Therefore it is likely that AEA synthesized during the cell stress can bind to Nav1.5 channel and modulate the actions of local anesthetics and class I antiarrhythmics with Nav1.5 channel. Although this, to our knowledge, is the first demonstration of the direct inhibitory action of AEA on a muscle type voltage-dependent Na⁺ channel, in several earlier investigations, AEA, at similar or higher concentrations, has been shown to inhibit directly the function of voltage-gated Na⁺ channels in neuronal structures (Kim *et al.*, 2005; Duan *et al.*, 2008; Theile and Cummins, 2011; Nicholson *et al.*, 2003). In agreement with our findings, both AEA (Theile and Cummins, 2011) and its metabolic product arachidonic acid (Bendahhou *et al.*, 1997) have been shown to increase inactivation of Na⁺ channels. Inhibition of VGSCs would slow the conduction of depolarization in the heart. However, it is unlikely that the slowed conduction due to Na⁺ channel inhibition alone would result in widening of QT interval observed in rat hearts (Farkas and Curtis, 2003).

In addition to I_{Na} , AEA caused a significant inhibition of cardiac $I_{L,Ca}$, which is mediated by Cav1.2 (gene CACNA1C) isoform of L-type VGCCs (Catterall *et al.*, 2005b). This current contributes to the plateau of the cardiac AP (phase 2), therefore, its suppression causes both the decrease of the amplitude of the plateau and the shortening of the AP duration. In earlier studies, AEA has been shown to decrease the amplitude of the plateau and cause shortening of the AP duration [(Li *et al.*, 2009; Al Kury *et al.*, 2014)]. Our results show that AEA affects activation and inactivation gating of cardiac L-

type VGCCs producing a significant reduction in $I_{L,Ca}$ “window current” in the range of V_m between -40 mV and +10 mV, and inducing partial blockade of the ion-conducting pathway leading to decreased amplitude of I_{Ca} .

Diminished stationary Ca^{2+} entry as a consequence of smaller “window current” may in part explain AEA-evoked enhancement of cardiomyocytes viability via prevention of Ca^{2+} overload and reduction of necrosis, whereas inhibition of $I_{L,Ca}$ may largely determine the decrease of the AP plateau amplitude and AP shortening observed in the presence of AEA. In cardiac muscle, extracellular Ca^{2+} required to trigger Ca^{2+} release from SR enters through L-type voltage-dependent Ca^{2+} channels opened during the AP. Collectively, these results suggest that during excitation-contraction coupling, the inhibition of L-type Ca^{2+} channels and the decrease in Ca^{2+} -induced Ca^{2+} release from sarcoplasmic reticulum causes negative inotropic effect of AEA reported in earlier studies. In line with this hypothesis, although caffeine-induced contractures and myofilament sensitivity to Ca^{2+} remained unchanged, electrically-induced Ca^{2+} transients were significantly depressed by AEA (Al Kury *et al.* 2014), further suggesting that Ca^{2+} -induced Ca^{2+} release was impaired in the presence of AEA. Overall, AEA-mediated suppression of voltage-activated $I_{L,Ca}$ would provide a mechanism for the negative inotropic effects observed in earlier studies.

Mechanism of the inhibitory effect of AEA does not seem to involve Ca^{2+} -induced inactivation process, since Ba^{2+} currents through L-type VGCCs were effectively inhibited by AEA. In addition, AEA was equally effective upon intracellular or extracellular application suggesting that there is no sidedness for AEA actions on L-type VGCCs. Considering highly lipophilic nature of AEA, it is not surprising that AEA can access its binding site from both extra and intracellular sites effectively. The results of radioligand binding and electrophysiological studies indicated that AEA directly interacts with and inhibits the function of L-type Ca^{2+} channels. Although, to our knowledge, this is the first

demonstration of the direct effects of AEA on the L-type VGCC in cardiac muscle, similar results demonstrating the effects AEA on skeletal muscle L-type VGCCs have also been described in biochemical studies (Oz *et al.*, 2000; Oz *et al.*, 2004). In our earlier studies in rabbit skeletal muscle, we have demonstrated that AEA inhibits the specific binding of [³H]Isradipine to skeletal T-tubule membranes and directly inhibits the functions of skeletal muscle L-type Ca²⁺ channels (Oz *et al.*, 2000; Oz *et al.*, 2004) in a manner that is independent of known cannabinoid receptors. In fact, earlier studies searching for endogenous modulators of L-type Ca²⁺ channels have also identified AEA as a ligand for L-type Ca²⁺ channels (Johnson *et al.*, 1993). Later investigations indicated that effects of AEA are not limited to L-type VGCCs in muscles, and other types of Ca²⁺ currents in neuronal structures are also inhibited directly by endocannabinoids such as AEA [for a recent review, (Lozovaya *et al.*, 2009)].

Involvement of cannabinoid-receptors in the negative inotropic actions of cannabinoids has been investigated in several earlier studies [for a recent review, (Batkai and Pacher, 2009)]. However, the results of these investigations have not been conclusive [for reviews, (Randall *et al.*, 2004; Mendizabal and Adler-Graschinsky, 2007; Malinowska *et al.*, 2012)]. Both cannabinoid receptor dependent and independent mechanisms have been suggested (Malinowska *et al.*, 2012). Experiments with AEA and the synthetic cannabinoid HU-210 performed in isolated Langendorff rat hearts and in isolated, electrically stimulated human atrial appendages (Ford *et al.*, 2002; Bonz *et al.*, 2003) have revealed a negative inotropic effect of cannabinoids that may underlie the ability of AEA and HU-210 to decrease cardiac output as observed in studies performed *in vivo* (Wagner *et al.*, 2001). In a recent study, it was found that a synthetic cannabinoid A-955840 inhibits the function of L-type Ca²⁺ channels in rabbit heart in a manner not sensitive to CB1 and CB2 antagonists (Su *et al.*, 2011). On the other hand, in another recent study, AEA was reported to inhibit L-type Ca²⁺ channels by the activation of CB1 receptors (Li *et al.*, 2009). In this study, AEA in the concentration range of 10 nM to 1 μM

potently inhibited the function of Ca^{2+} channels and the effect of AEA was reversed by CB1 receptor antagonists. In our experiments, AEA was not effective at concentration lower than 1 μM . In addition, in our study, the inhibitory effect of AEA was not reversed by the antagonists of CB1 and CB2 receptors. Differences between two studies could be due to different strains of rats used (Sprague-Dawley in their study versus Wistar rats in the present study). Our findings suggest that neither CB1 nor CB2 receptors are involved in AEA inhibition of L-type Ca^{2+} channels in rat cardiomyocytes.

Although PTX-sensitive signal transduction is well documented for cannabinoid agonists, cannabinoid coupling to PTX-insensitive G_q has been reported in several studies (McIntosh *et al.*, 2007; Straiker *et al.*, 2002; Ishii and Chun, 2002). Therefore, the effect of AEA through PTX-insensitive pathway cannot be excluded.

AEA belongs to a group of fatty acid-based molecules called long-chain N-acylethanolamines (NAEs) which are produced abundantly in response to tissue necrosis and cellular stress (Hansen *et al.*, 2000; Berger *et al.*, 2004). In fact, accumulation of NAEs was first observed in experimental myocardial infarction induced by ligation of coronary arteries in canine heart [(Epps *et al.*, 1979; Epps *et al.*, 1982) for a review, (Schmid and Berdyshev, 2002)]. It was demonstrated that NAE content increases up to 500 nmol/g (approximately 500 μM) in infarcted areas of canine heart during ischemia (Epps *et al.*, 1979). Although AEA constitutes minor (1-3 %) portion of total NAE levels (Schmid and Berdyshev, 2002), the results of this study may have important implications regarding the contractile responses of ventricular myocytes to ischemia and cellular stress (Hansen *et al.*, 2000; Schmid and Berdyshev, 2002; Berger *et al.*, 2004). We have previously reported that major NAEs species including AEA produced during ischemia have significant effects on the amplitudes and kinetics of action potentials and accompanying ionic currents that could account for the negative inotropic actions of these compounds on ventricular myocytes (Voitychuk *et al.*, 2012). For example, functions of voltage-gated Ca^{2+} (Oz *et*

al., 2000); (Oz *et al.*, 2004; Oz *et al.*, 2005; Alptekin *et al.*, 2010; Voitychuk *et al.*, 2012) and Na⁺ (Voitychuk *et al.*, 2012; Gulaya *et al.*, 1993) channels have been demonstrated to be modulated by NAEs. In the concentration range used in our study, AEA has been shown to inhibit the function of various cardiac ion channels in cannabinoid receptor- independent manner. For example, AEA blocks T- type Ca²⁺ channels (Cav3.1 and Cav 3.2) (Chemin *et al.*, 2007) and cardiac Kv1.5 (Barana *et al.*, 2010) and Kv4.3 (Amoros *et al.*, 2010) in a receptor- independent manner. These effects may contribute to the overall effects of AEA on action potential and myocyte function.

In conclusion, the results indicate for the first time that AEA interacts directly with Na⁺ and L-type Ca²⁺ channels in ventricular myocytes in a manner that is independent of CB1 and CB2 receptors.

Acknowledgments: This study was in supported by the NIDA/NIH, USA and the United Arab Emirates University Research Funds. We thank Mr. Anwar Qureshi for his excellent technical help in isolating rat ventricular myocytes.

Statement of conflict of interest: The authors declare no conflict of interest.

Author contributions:

Petro Doroshenko, Yaroslav M. Shuba, Sehamuddin Galadari, Frank Christopher Howarth, Murat Oz: contributed the design of experiments, analyzed data and also contributed to writing of the article.

Reference List

- Abadji V, Lin S, Taha G, Griffin G, Stevenson LA, Pertwee RG *et al.* (1994). (R)-methanandamide: a chiral novel anandamide possessing higher potency and metabolic stability. *J Med Chem* 37: 1889-1893.
- Alexander SP, Mathie A, Peters JA (2011). *Guide to Receptors and Channels (GRAC)*, 5th edition. *Br J Pharmacol*, 164 (Suppl. 1): S1-S324.
- Al Kury LT, Voitychuk OI, Ali RM, Galadari S, Yang KH, Howarth FC *et al.* (2014). Effects of endogenous cannabinoid anandamide on excitation-contraction coupling in rat ventricular myocytes. *Cell Calcium* 55: 104-118.
- Alptekin A, Galadari S, Shuba Y, Petroianu G, Oz M (2010). The effects of anandamide transport inhibitor AM404 on voltage-dependent calcium channels. *Eur J Pharmacol* 634: 10-15.
- Amoros I, Barana A, Caballero R, Gomez R, Osuna L, Lillo MP *et al.* (2010). Endocannabinoids and cannabinoid analogues block human cardiac Kv4.3 channels in a receptor-independent manner. *J Mol Cell Cardiol* 48: 201-210.
- Andrag E, Curtis, MJ (2013). Feasibility of targeting ischaemia-related ventricular arrhythmias by mimicry of endogenous protection by endocannabinoids. *Br J Pharmacol* 169: 1840-1848.
- Barana A, Amoros I, Caballero R, Gomez R, Osuna L, Lillo MP (2010). Endocannabinoids and cannabinoid analogues block cardiac hKv1.5 channels in a cannabinoid receptor-independent manner. *Cardiovasc Res* 85: 56-67.
- Batkai S, Pacher P (2009). Endocannabinoids and cardiac contractile function: pathophysiological implications. *Pharmacol Res* 60: 99-106.
- Bebarova M, Matejovic P, Pasek M, Ohlidalova D, Jansova D, Simurdova M *et al.* (2010). Effect of ethanol on action potential and ionic membrane currents in rat ventricular myocytes. *Acta Physiol (Oxf)* 200: 301-314.
- Bendahhou S, Cummins TR, Agnew WS (1997). Mechanism of modulation of the voltage-gated skeletal and cardiac muscle sodium channels by fatty acids. *Am J Physiol* 272: C592-C600.
- Berger C, Schmid PC, Schabitz WR, Wolf M, Schwab S, Schmid HH (2004). Massive accumulation of N-acyl ethanolamines after stroke. Cell signalling in acute cerebral ischemia? *J Neurochem* 88: 1159-1167.
- Bonz A, Laser M, Kullmer S, Kniesch S, Babin-Ebell J, Popp V *et al.* (2003). Cannabinoids acting on CB1 receptors decrease contractile performance in human atrial muscle. *J Cardiovasc Pharmacol* 41: 657-664.
- Bouchard JF, Lepicier P, Lamontagne D (2003). Contribution of endocannabinoids in the endothelial protection afforded by ischemic preconditioning in the isolated rat heart. *Life Sci* 72: 1859-1870.

Catterall WA, Goldin AL, Waxman SG. (2005a). International Union of Pharmacology. XLVII. Nomenclature and structure-function relationships of voltage-gated sodium channels. *Pharmacol Rev* 57: 397-409.

Catterall WA, Perez-Reyes E, Snutch TP, Striessnig J (2005b). International Union of Pharmacology. XLVIII. Nomenclature and structure-function relationships of voltage-gated calcium channels. *Pharmacol Rev* 57: 411-425.

Chemin J, Nargeot J, Lory, P (2007). Chemical determinants involved in anandamide-induced inhibition of T-type calcium channels. *J Biol Chem* 282: 2314-2323.

Danziger RS, Sakai M, Capogrossi MC, Spurgeon HA, Hansford RG, Lakatta, EG (1991). Ethanol acutely and reversibly suppresses excitation-contraction coupling in cardiac myocytes. *Circ Res* 68: 1660-1668.

Di Marzo V, De Petrocellis L, Bisogno, T (2005). The biosynthesis, fate and pharmacological properties of endocannabinoids. *Handb Exp Pharmacol*: 147-185.

Duan Y, Zheng J, Nicholson RA (2008). Inhibition of [3H]batrachotoxinin A-20 α -benzoate binding to sodium channels and sodium channel function by endocannabinoids. *Neurochem Int* 52: 438-446.

Dunn SM (1989). Voltage-dependent calcium channels in skeletal muscle transverse tubules. Measurements of calcium efflux in membrane vesicles. *J Biol Chem* 264: 11053-11060.

Epps DE, Mandel F, Schwartz, A (1982). The alteration of rabbit skeletal sarcoplasmic reticulum function by N-acylethanolamine, a lipid associated with myocardial infarction. *Cell Calcium* 3: 531-543.

Epps DE, Schmid PC, Natarajan V, Schmid HH (1979). N-Acylethanolamine accumulation in infarcted myocardium. *Biochem Biophys Res Commun* 90: 628-633.

Farkas A, Curtis, MJ (2003). Does QT widening in the Langendorff-perfused rat heart represent the effect of repolarization delay or conduction slowing? *J Cardiovasc Pharmacol* 42: 612-621.

Ford WR, Honan SA, White R, Hiley, CR (2002). Evidence of a novel site mediating anandamide-induced negative inotropic and coronary vasodilator responses in rat isolated hearts. *Br J Pharmacol* 135: 1191-1198.

Gulaya NM, Melnik AA, Balkov DI, Volkov GL, Vysotskiy MV, Vaskovsky VE (1993). The effect of long-chain N-acylethanolamines on some membrane-associated functions of neuroblastoma C1300 N18 cells. *Biochim Biophys Acta* 1152: 280-288.

Hansen HS, Moesgaard B, Hansen HH, Petersen G (2000). N-Acylethanolamines and precursor phospholipids - relation to cell injury. *Chem Phys Lipids* 108: 135-150.

Hanus LO, Mechoulam R (2010). Novel natural and synthetic ligands of the endocannabinoid system. *Curr Med Chem* 17: 1341-1359.

Howarth FC, Qureshi MA, White E (2002). Effects of hyperosmotic shrinking on ventricular myocyte shortening and intracellular Ca(2+) in streptozotocin-induced diabetic rats. *Pflugers Arch* 444: 446-451.

Ishii I, Chun, J (2002). Anandamide-induced neuroblastoma cell rounding via the CB1 cannabinoid receptors. *Neuroreport* 13: 593-596.

Johnson DE, Heald SL, Dally RD, Janis RA. (1993). Isolation, identification and synthesis of an endogenous arachidonic amide that inhibits calcium channel antagonist 1,4-dihydropyridine binding. *Prostaglandins Leukot Essent Fatty Acids* 48: 429-437.

Kang JX, Leaf A (1996). Evidence that free polyunsaturated fatty acids modify Na⁺ channels by directly binding to the channel proteins. *Proc Natl Acad Sci U S A* 93: 3542-3546.

Kilkenny C, Browne WJ, Cuthill IC, Emerson M, Altman, DG. (2010). Improving bioscience research reporting: The ARRIVE guidelines for reporting animal research. *J Pharmacol Pharmacother* 1: 94-99.

Kim HI, Kim TH, Shin YK, Lee CS, Park M, Song, JH. (2005). Anandamide suppression of Na⁺ currents in rat dorsal root ganglion neurons. *Brain Res* 1062: 39-47.

Krylatov AV, Uzhachenko RV, Maslov LN, Bernatskaya NA, Makriyannis A, Mechoulam R (2002). Endogenous cannabinoids improve myocardial resistance to arrhythmogenic effects of coronary occlusion and reperfusion: a possible mechanism. *Bull Exp Biol Med* 133: 122-124.

Lan R, Liu Q, Fan P, Lin S, Fernando SR, McCallion D *et al.* (1999). Structure-activity relationships of pyrazole derivatives as cannabinoid receptor antagonists. *J Med Chem* 42: 769-776.

Li Q, Ma HJ, Zhang H, Qi Z, Guan Y, Zhang Y (2009). Electrophysiological effects of anandamide on rat myocardium. *Br J Pharmacol* 158: 2022-2029.

Lozovaya N, Min R, Tsintsadze V, Burnashev N (2009). Dual modulation of CNS voltage-gated calcium channels by cannabinoids: Focus on CB1 receptor-independent effects. *Cell Calcium* 46: 154-162.

Malinowska B, Baranowska-Kuczko M, Schlicker E (2012). Triphasic blood pressure responses to cannabinoids: do we understand the mechanism? *Br J Pharmacol* 165: 2073-2088.

McGrath JC, Drummond GB, McLachlan EM, Kilkenny C, Wainwright CL (2010). Guidelines for reporting experiments involving animals: the ARRIVE guidelines. *Br J Pharmacol* 160: 1573-1576.

McIntosh BT, Hudson B, Yegorova S, Jollimore CA, Kelly ME (2007). Agonist-dependent cannabinoid receptor signalling in human trabecular meshwork cells. *Br J Pharmacol* 152: 1111-1120.

Mendizabal VE, Adler-Graschinsky E (2007). Cannabinoids as therapeutic agents in cardiovascular disease: a tale of passions and illusions. *Br J Pharmacol* 151: 427-440.

Montecucco F, Di Marzo, V (2012). At the heart of the matter: the endocannabinoid system in cardiovascular function and dysfunction. *Trends Pharmacol Sci* 33: 331-340.

Nicholson RA, Liao C, Zheng J, David LS, Coyne L, Errington AC (2003). Sodium channel inhibition by anandamide and synthetic cannabimimetics in brain. *Brain Res* 978: 194-204.

Oz M (2006). Receptor-independent actions of cannabinoids on cell membranes: focus on endocannabinoids. *Pharmacol Ther* 111: 114-144.

Oz M, Alptekin A, Tchugunova Y, Dinc M (2005). Effects of saturated long-chain N-acylethanolamines on voltage-dependent Ca²⁺ fluxes in rabbit T-tubule membranes. *Arch Biochem Biophys* 434: 344-351.

Oz M, Tchugunova Y, Dinc, M (2004). Differential effects of endogenous and synthetic cannabinoids on voltage-dependent calcium fluxes in rabbit T-tubule membranes: comparison with fatty acids. *Eur J Pharmacol* 502: 47-58.

Oz M, Tchugunova YB, Dunn SM (2000). Endogenous cannabinoid anandamide directly inhibits voltage-dependent Ca(2+) fluxes in rabbit T-tubule membranes. *Eur J Pharmacol* 404: 13-20.

Pacher P, Batkai S, Kunos, G (2006). The endocannabinoid system as an emerging target of pharmacotherapy. *Pharmacol Rev* 58: 389-462.

Pertwee RG, Howlett AC, Abood ME, Alexander SP, Di Marzo V, Elphick MR (2010). International Union of Basic and Clinical Pharmacology. LXXIX. Cannabinoid receptors and their ligands: beyond CB and CB. *Pharmacol Rev* 62: 588-631.

Postma SW, Catterall WA (1984). Inhibition of binding of [3H]batrachotoxinin A 20- α -benzoate to sodium channels by local anesthetics. *Mol Pharmacol* 25: 219-227.

Randall MD, Kendall DA, O'Sullivan S (2004). The complexities of the cardiovascular actions of cannabinoids. *Br J Pharmacol* 142: 20-26.

Ross RA, Brockie HC, Stevenson LA, Murphy VL, Templeton F, Makriyannis A *et al.* (1999). Agonist-inverse agonist characterization at CB1 and CB2 cannabinoid receptors of L759633, L759656, and AM630. *Br J Pharmacol* 126: 665-672.

Schmid HH, Berdyshev EV (2002). Cannabinoid receptor-inactive N-acylethanolamines and other fatty acid amides: metabolism and function. *Prostaglandins Leukot Essent Fatty Acids* 66: 363-376.

Sheldon RS, Cannon NJ, Duff HJ (1986). Binding of [3H]batrachotoxinin A benzoate to specific sites on rat cardiac sodium channels. *Mol Pharmacol* 30: 617-623.

Sheldon RS, Duff HJ, Thakore E, Hill RJ (1994). Class I antiarrhythmic drugs: allosteric inhibitors of [3H] batrachotoxinin binding to rat cardiac sodium channels. *J Pharmacol Exp Ther* 268: 187-194.

Soldatov NM, Oz M, O'Brien KA, Abernethy DR, Morad, M (1998). Molecular determinants of L-type Ca²⁺ channel inactivation. Segment exchange analysis of the carboxyl-terminal cytoplasmic motif encoded by exons 40-42 of the human α 1C subunit gene. *J Biol Chem* 273: 957-963.

Straiker AJ, Borden CR, Sullivan JM (2002). G-protein α subunit isoforms couple differentially to receptors that mediate presynaptic inhibition at rat hippocampal synapses. *J Neurosci* 22: 2460-2468.

Su Z, Preusser L, Diaz G, Green J, Liu X, Polakowski J *et al.* (2011). Negative inotropic effect of a CB2 agonist A-955840 in isolated rabbit ventricular myocytes is independent of CB1 and CB2 receptors. *Curr Drug Saf* 6: 277-284.

Theile JW, Cummins TR (2011). Inhibition of Nav β 4 peptide-mediated resurgent sodium currents in Nav1.7 channels by carbamazepine, riluzole, and anandamide. *Mol Pharmacol* 80: 724-734.

Ugdyzhekova DS, Bernatskaya NA, Stefano JB, Graier VF, Tam SW, Mekhoulam R (2001). Endogenous cannabinoid anandamide increases heart resistance to arrhythmogenic effects of epinephrine: role of CB(1) and CB(2) receptors. *Bull Exp Biol Med* 131: 251-253.

Voitychuk OI, Asmolkova VS, Gula NM, Sotkis GV, Galadari S, Howarth FC *et al.* (2012). Modulation of excitability, membrane currents and survival of cardiac myocytes by N-acylethanolamines. *Biochim Biophys Acta* 1821: 1167-1176.

Wagner JA, Jarai Z, Batkai S, Kunos G (2001). Hemodynamic effects of cannabinoids: coronary and cerebral vasodilation mediated by cannabinoid CB(1) receptors. *Eur J Pharmacol* 423: 203-210.

Zhang ZS, Cheng HJ, Onishi K, Ohte N, Wannenburg T, Cheng CP (2005). Enhanced inhibition of L-type Ca $^{2+}$ current by β 3-adrenergic stimulation in failing rat heart. *J Pharmacol Exp Ther* 315: 1203-1211.

Accepted Article

FIGURE LEGENDS

Fig. 1: Effect of AEA on voltage-dependent Na⁺ currents (I_{Na}) in rat ventricular myocytes.

(A) AEA inhibits I_{Na} recorded using whole cell voltage clamp mode of patch clamp technique. I_{Na} was recorded during 50 ms voltage pulses to -20 mV from a holding potential of -80 mV. Current traces were recorded before (control) and after 10 min application of 10 μ M AEA. (B) Maximal currents of VGSCs presented as a function of time in the presence of vehicle (0.07% ethanol) and 10 μ M AEA (n=5-6 cells). (C) Representative recordings of I_{Na} in response to the depicted pulse protocol under control conditions and after application of 10 μ M AEA. (D) Normalized and averaged I - V relationships of control I_{Na} (filled circles) and I_{Na} in the presence of 10 μ M AEA (open circles) determined by applying a series of step depolarizing pulses from -80 mV to +70 mV in 10 mV increments for a duration of 50 ms. Data points (mean \pm S.E.M.) are from 5 to 7 cells.

Fig. 2: Effect of AEA on steady state activation and inactivation of I_{Na} and of pertussis toxin pretreatment on AEA inhibition of I_{Na} in rat ventricular myocytes .

(A) Steady-state activation (SSA) and (B) steady-state inactivation (SSI) curves of I_{Na} in the absence (filled circles) and presence of 1 μ M AEA (open circles). Fit of experimental data points with Boltzmann equation (see text for parameters). (C) Voltage-dependence of I_{Na} inactivation time constant (τ_i) under control conditions (filled circles) and in the presence of 1 μ M AEA (open circles). Data points (mean \pm S.E.M.) are from 5 cells. (D) Effect of PTX pretreatment on AEA inhibition of the maximal I_{Na} amplitudes. Black bars indicate controls. Bars present mean \pm S.E.M. from 5-8 cells.

Fig. 3: Effects of metAEA and cannabinoid receptor antagonists AM251 and AM630 on the specific binding of [³H]BTX-B to rat ventricular myocytes.

(A) Specific binding as a function of the concentration of [³H]BTX-B in the absence and presence of metAEA. Data points for controls and metAEA (10 μ M) are indicated by filled circles and open circles, respectively. (B)

Scatchard analysis of the effects of metAEA on saturation binding of [^3H]BTX-B to ventricular myocytes. The slope and intercept of the linear regression curve indicate the K_D and B_{max} values, respectively. Data points were determined from a set of binding experiments presented in the panel A. (C) Effect of increasing metAEA concentration on the specific binding of [^3H]BTX-B to ventricular myocytes. Binding was measured as described in the methods. Data are the means of 5-6 experiments. (D) Effects of cannabinoid receptor antagonists AM251 (1 μM) and AM630 (1 μM) and their co-application with metAEA (10 μM) on the specific binding of [^3H]BTX-B to cardiomyocytes. Bars present mean \pm S.E.M. from 7-11 cells.

Fig. 4: Effect of AEA on Ca^{2+} currents mediated by L-type Ca^{2+} channels in rat ventricular myocytes.

(A) AEA inhibits L-type Ca^{2+} currents recorded using whole-cell voltage-clamp mode of patch clamp technique. Current traces recorded before (control) and after 10 min application of 1 μM AEA. I_{Ca} were recorded during 300 ms voltage pulses to +10 mV from a holding potential of -50 mV. (B) Averages of the maximal currents of VGCCs presented as a function of time in the presence of vehicle and 1 μM AEA (n=5 cells; filled circles). Application time for the agents was presented in a horizontal bar. (C) Representative recordings of I_{Ca} in response to the depicted pulse protocol under control conditions and after application of 1 μM AEA. (D) Normalized and averaged I - V relationships of control I_{Ca} (open circles) and I_{Ca} in the presence of 10 μM AEA (filled circles) determined by applying a series of step depolarizing pulses from -70 mV to +70 mV in 10 mV increments for a duration of 300 ms. Data points (mean \pm S.E.M.) are from 5 to 7 cells.

Fig. 5: Effect of AEA on steady state activation and inactivation of I_{Ca} and of sidedness of AEA application on I_{Ca} in rat ventricular myocytes.

(A) Steady-state activation (SSA) and (B) steady-state inactivation (SSI) curves of I_{Ca} in the absence (open circles) and presence of 1 μM AEA (filled circles). Data points (mean \pm S.E.M.) are from 5 cells. Fit of experimental data points with Boltzmann equation. (C) Voltage-dependent fast (triangles) and slow (circles) inactivation time constants (τ_i) of $I_{\text{L,Ca}}$ under control conditions (filled circles, and triangles) and in the presence of 1 μM AEA (open circles and triangles). Data points (mean \pm S.E.M.) are from 5-6 cells. (D) Comparison of the

intracellular and extracellular application of AEA on the maximal inhibition of I_{Ca} . Bars present mean \pm S.E.M. from 5-8 cells.

Fig. 6: Effect of AEA on Ba^{2+} currents mediated by L-type Ca^{2+} channels, and effects of pertussis toxin pretreatment and cannabinoid receptor antagonists on AEA inhibition of L-type Ca^{2+} channels.

(A) Traces of normalized Ca^{2+} and Ba^{2+} currents through L-type VGCCS. Normalized Ba^{2+} current in the presence 1 μ M AEA was presented in the figure. (B) Effect of 1 μ M AEA on the maximal amplitudes and the inactivation kinetics of Ba^{2+} currents. Bars present mean \pm S.E.M. from 7-8 cells. (C) Percent inhibition of L-type Ca^{2+} currents after vehicle (DW) and PTX (2 μ g/ μ l, 3hours). Bars present mean \pm S.E.M. from 6-8 cells. (D) Effects of CB1 antagonist AM251 (0.3 μ M) and CB2 antagonist AM630 (0.3 μ M) on AEA (1 μ M) inhibition of L-type Ca^{2+} currents. Bars present mean \pm S.E.M. from 6-9 cells

Fig. 7: Effects of metAEA and cannabinoid receptor antagonists AM251 and AM630 on the specific binding of [3 H]Isradipine to rat ventricular muscle membranes.

(A) Specific binding as a function of the concentration of [3 H]Isradipine in the absence and presence of metAEA. Data points for controls and metAEA (10 μ M) are indicated by filled and open circles, respectively. (B) Scatchard analysis of the effects of metAEA on saturation binding of [3 H]Isradipine binding to cardiac muscle membranes. The slope and intercept of the linear regression curve indicate the K_D and B_{max} values, respectively. Data points were determined from a set of binding experiment presented in the panel A. (C) Effects of increasing the concentration of metAEA on the specific binding of [3 H]Isradipine to cardiac muscle membranes. Data are the means of 5-6 experiments. (D) Effects of cannabinoid receptor antagonists AM251 (1 μ M) and AM630 (1 μ M)) and their co-application with metAEA (10 μ M) on the specific binding of [3 H]Isradipine to T-tubule membranes. Bars present mean \pm S.E.M. from 5-6 experiments.

SUPPLEMENTS:

Supplement Fig. 1: Effect of increasing AEA and vehicle (ethanol) concentrations on the voltage-activated sodium currents recorded in rat ventricular myocytes.

(A) Effects of AEA (0.1 to 30 μM) and corresponding vehicle concentrations on the maximal amplitudes of I_{Na} currents. Each bar represents mean \pm S.E.M. from 5 to 7 cells (B) Corrected concentration response curve for the inhibitory effect of AEA on I_{Na} . The amount of inhibition induced by the vehicle was subtracted from the AEA-induced inhibition at corresponding AEA concentrations. Data was fit with logistic equation using Origin data analysis software.

Supplement Fig. 2: Effect of pertussis toxin (PTX) pretreatment on BRL-37344 inhibition of voltage activated Ca^{2+} currents (I_{Ca}) recorded in rat ventricular myocytes.

(A) Records of currents presenting the effect of BRL-37344, a β_3 adrenergic receptor agonist, on I_{Ca} in the absence and presence of PTX (2 $\mu\text{g}/\text{ml}$ for 3 hours in 37 $^{\circ}\text{C}$) pretreatment. Records were obtained by applying a step depolarizing pulse from -50 mV to +20 mV for a duration of 300 ms (B) Presentation of results on the effect of PTX pretreatment on BRL-37344 inhibition of I_{Ca} . Each bar presents mean \pm S.E.M. from 5-7 cells.* indicates statistically significant difference at the level of $P < 0.05$.

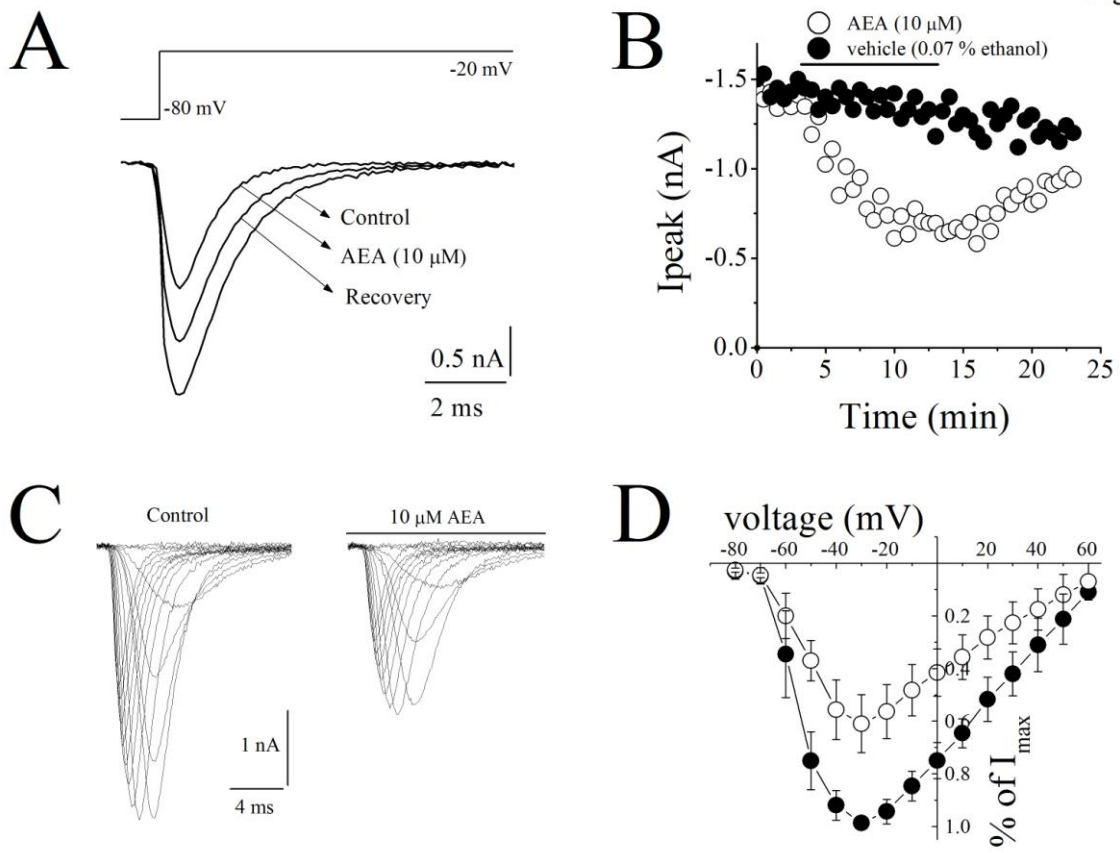
Supplement Fig. 3: Effects of increasing AEA and vehicle (ethanol) concentrations on the L-type voltage-activated Ca^{2+} currents ($I_{\text{L,Ca}}$) recorded in rat ventricular myocytes.

(A) Effects of AEA (0.1 to 30 μM) and corresponding vehicle concentrations on the maximal amplitudes of $I_{\text{L,Ca}}$. Each bar represents mean \pm S.E.M. from 5 to 7 cells (B) Corrected concentration response curve for the inhibitory effect of AEA on $I_{\text{L,Ca}}$. The amount of inhibition induced by the vehicle was subtracted from the AEA-induced inhibition at corresponding AEA concentrations. Data was fit with logistic equation using Origin data analysis software. Application of AEA inhibited $I_{\text{L,Ca}}$ in a concentration-dependent manner with an $\text{IC}_{50} =$

10.2±0.6 iM, slope factor of 36±0.2, but two-fold higher efficacy (i.e., maximal block at saturating concentration $\lambda=72.0\pm2.9\%$) compared to I_{Na} (see supplement figure 1B for comparison).

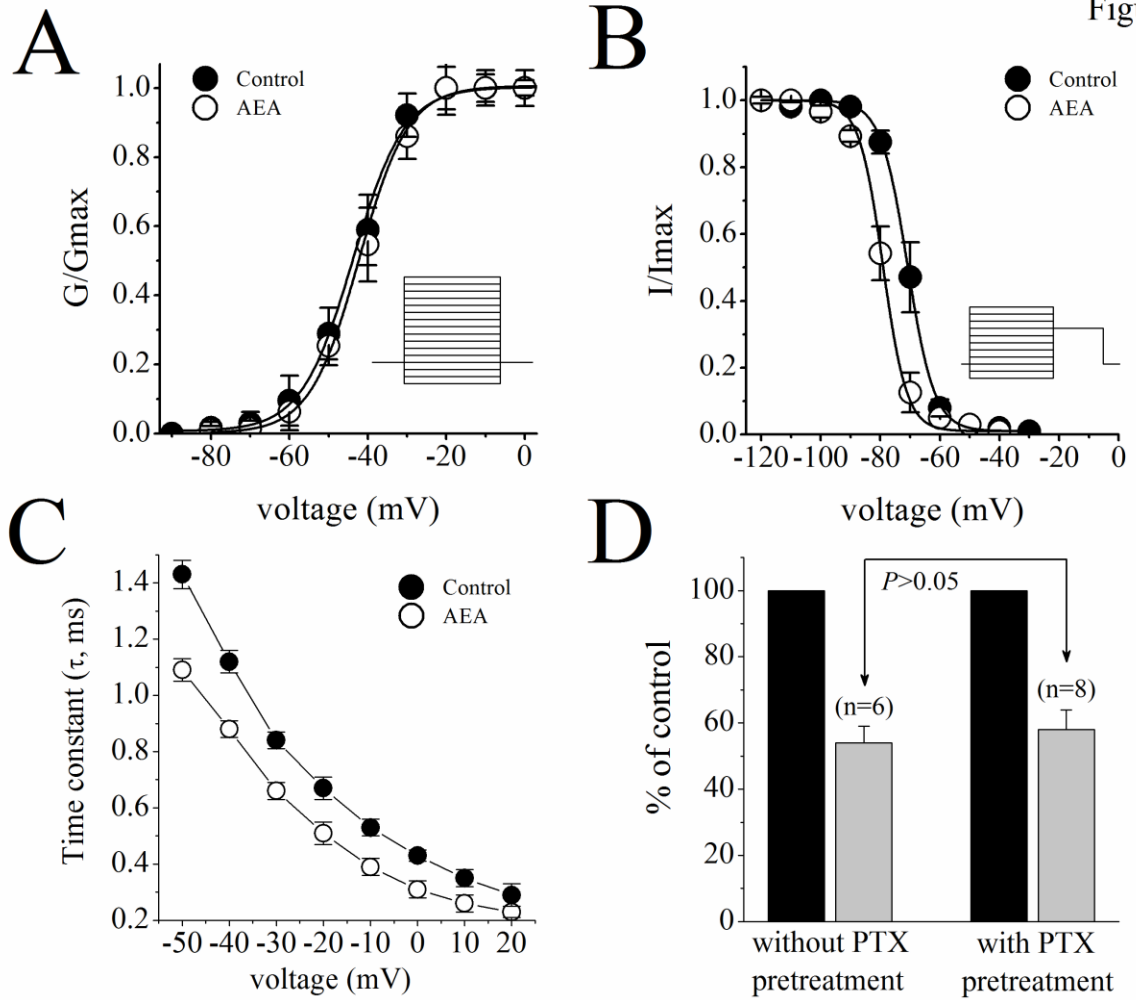
Accepted Article

Figure 1



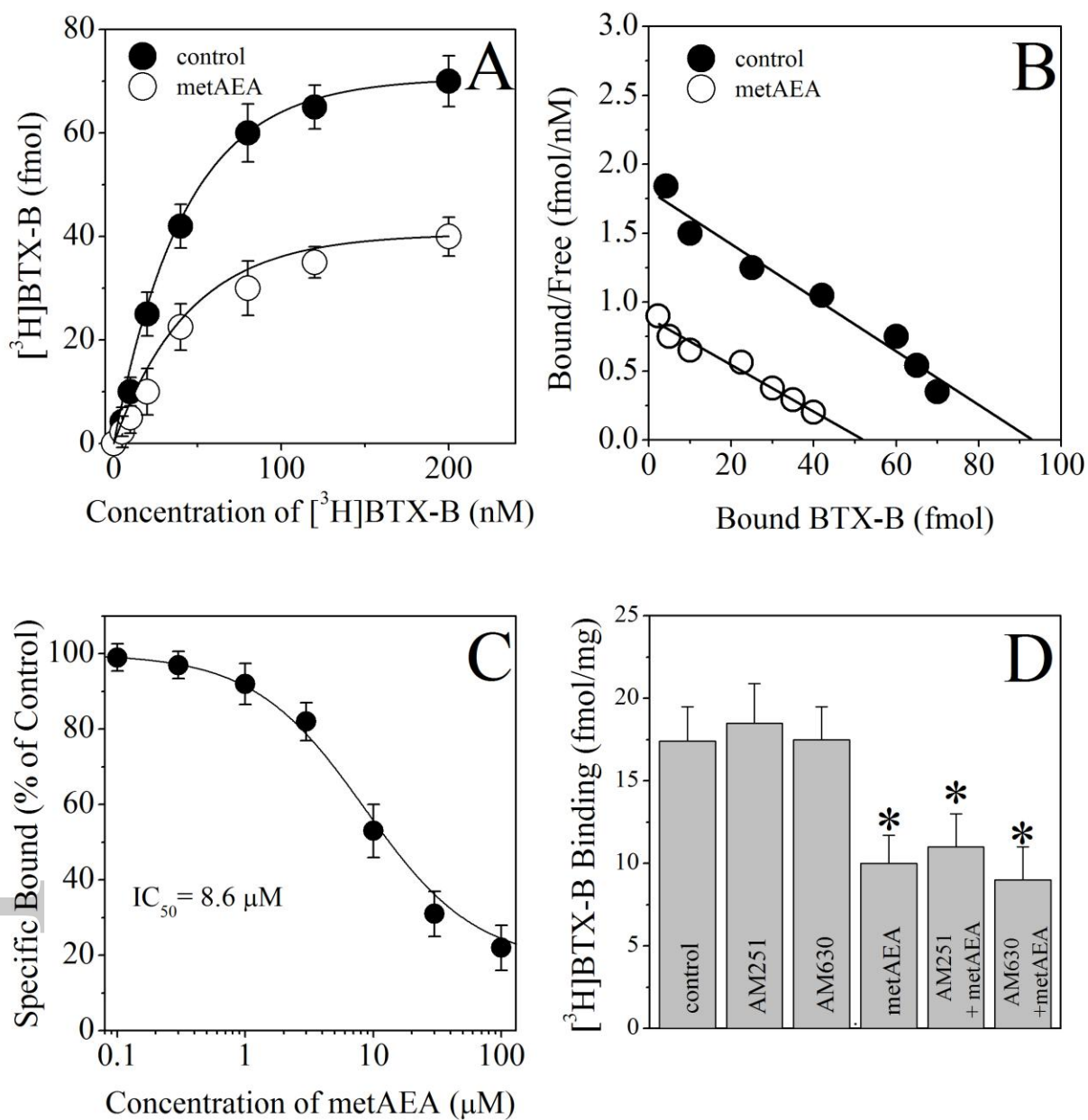
bph_12734_f1

Figure 2



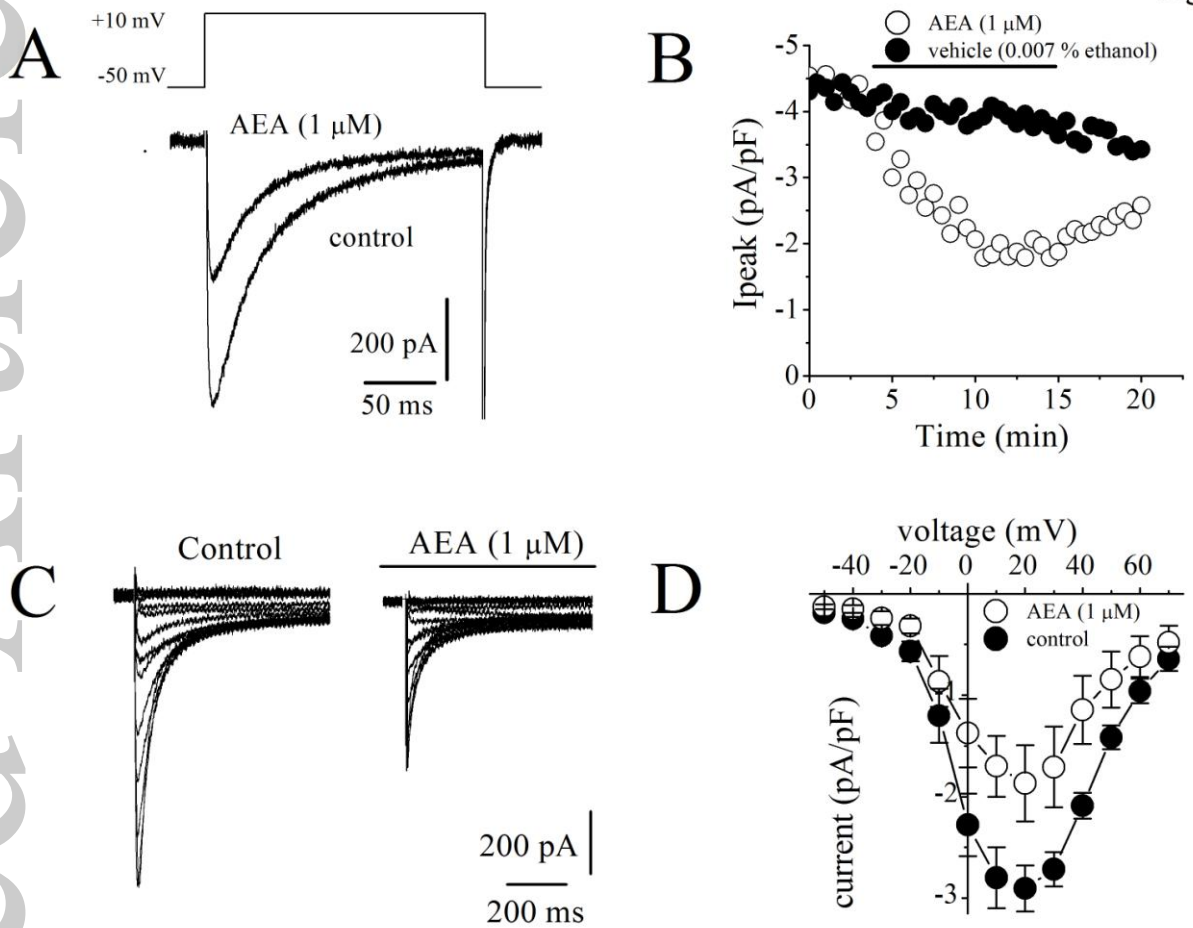
bph_12734_f2

Figure 3



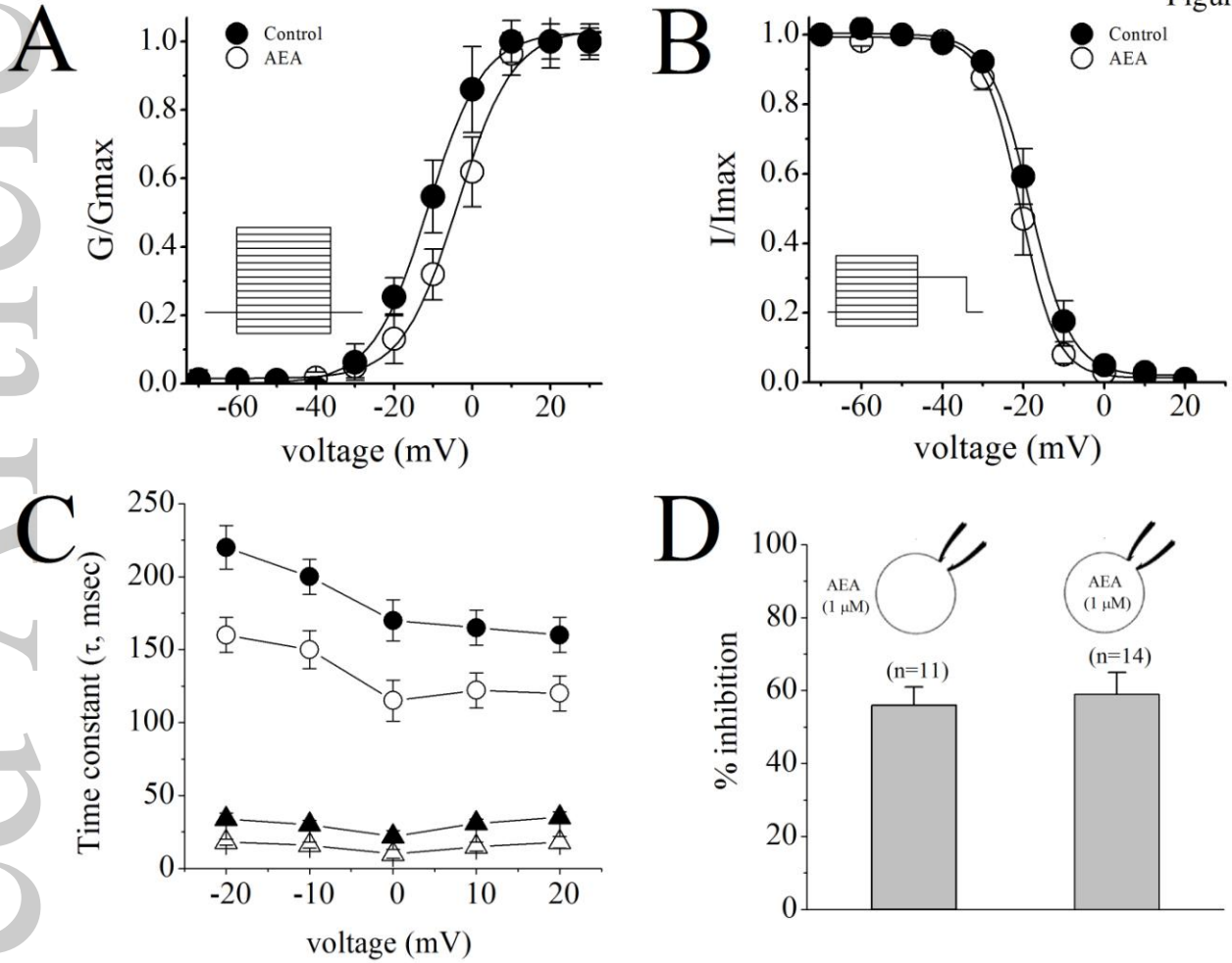
bph_12734_f3

Figure 4



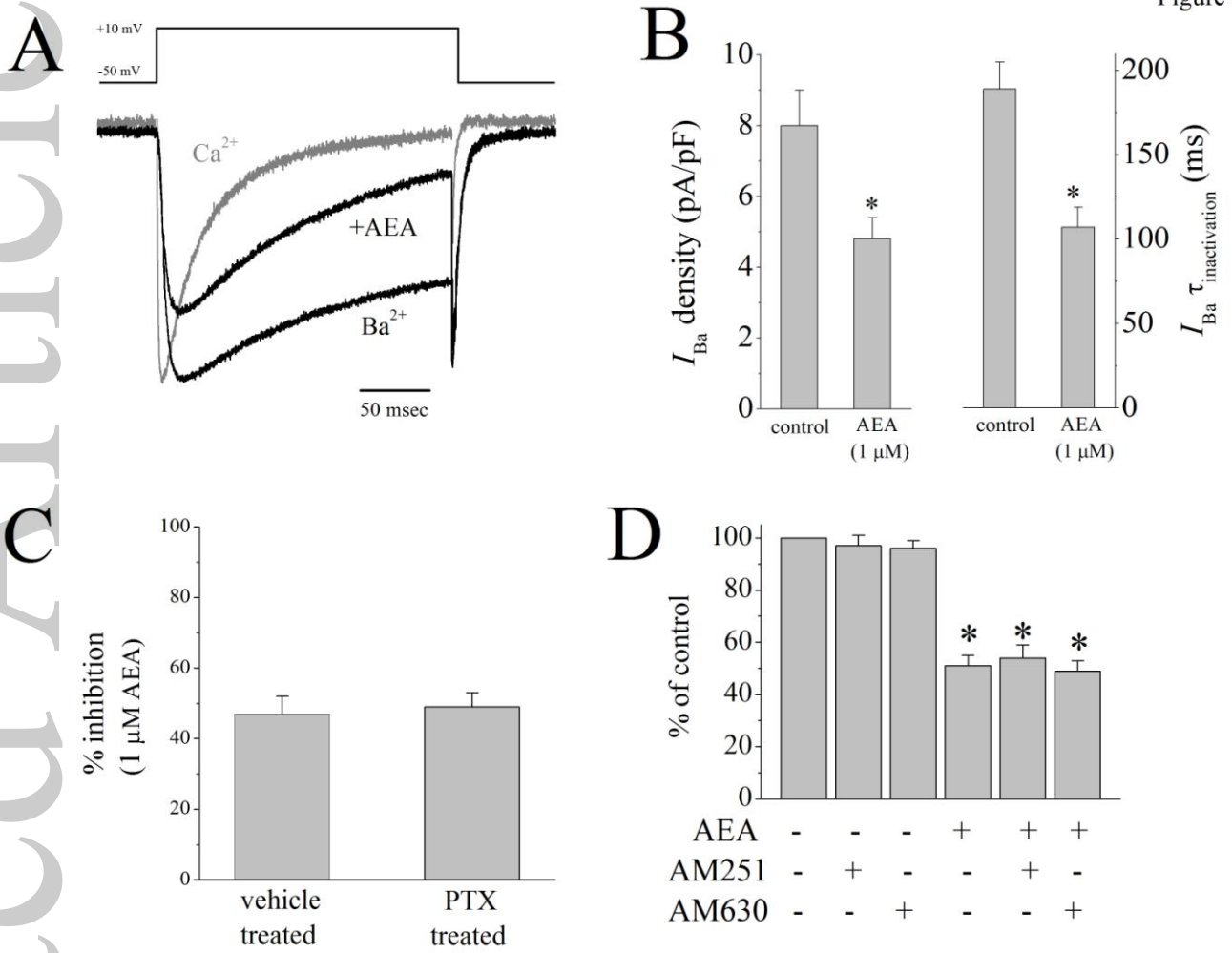
bph_12734_f4

Figure 5



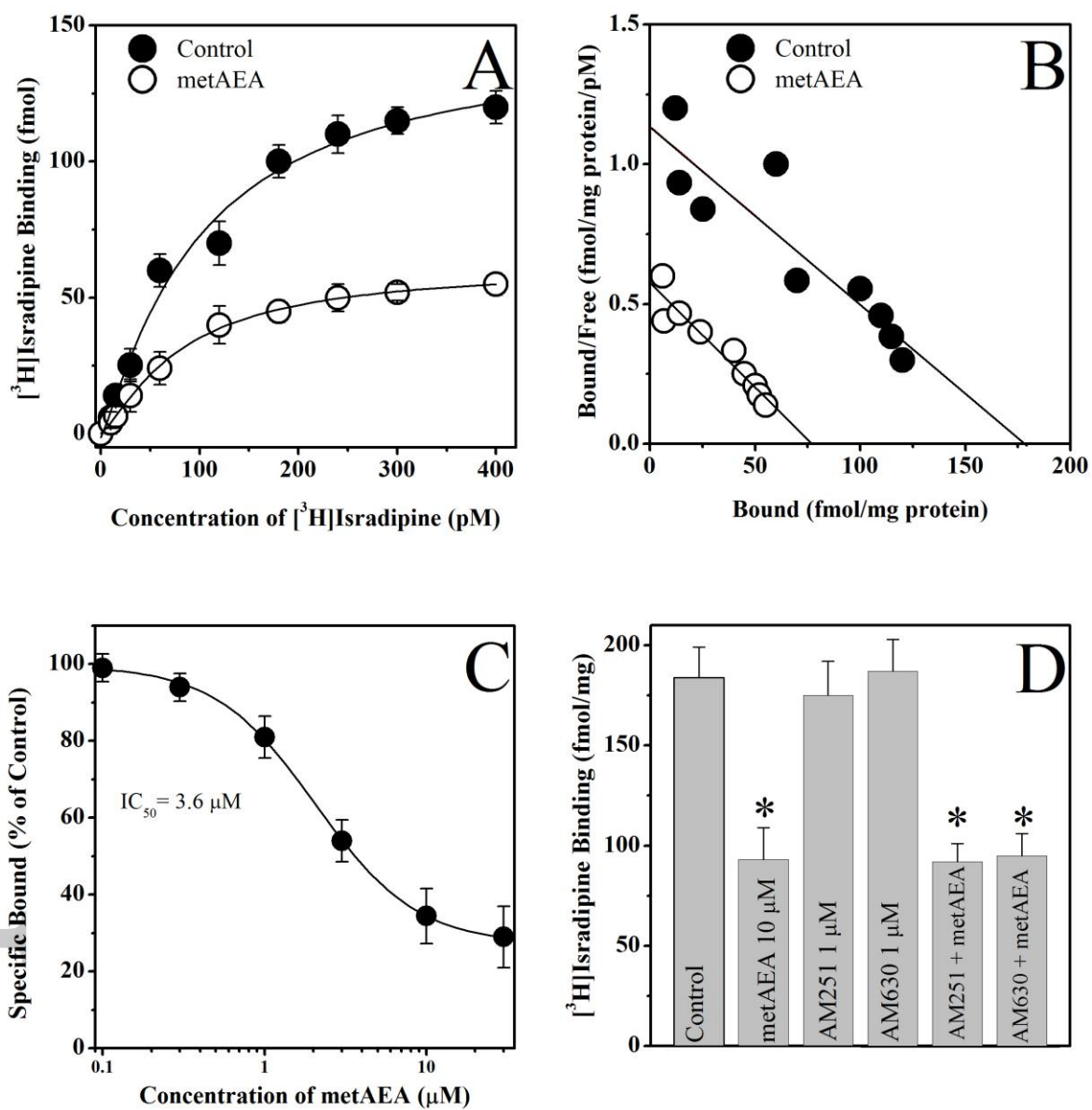
bph_12734_f5

Figure 6



bph_12734_f6

Figure 7



bph_12734_f7